19th Symposium IMEKO TC 4 Symposium and 17th IWADC Workshop
Advances in Instrumentation and Sensors Interoperability
July 18-19, 2013, Barcelona, Spain

Study of a Hall Effect Brake Wear Sensor using Finite Element Modelling and Analysis

Anoop C. S., Boby George

Indian Institute of Technology, Chennai, India, +91442254465, boby@ee.iitm.ac.in

Abstract-Monitoring of brake wear and warning the driver to replace it at the appropriate time is a critical safety requirement. Recently, basic concept of a new, simple and low-cost Hall-Effect (HE) based angle sensor, which continuously monitors brake wear, by sensing the angle rotated by the Cam Shaft (CS) with-respect-to the Slack Adjuster (SA) in the brake assembly has been presented. The sensor has a spiral shaped moving part. It rotates along with CS, and changes the magnetic field seen by a HE sensor, whose output is directly proportional to angle between CS and SA, for a wide range. A prototype angle sensor has been developed, and test results showed a linear range of 220º, which is sufficient for monitoring brake wear. In the sensor, parameters like positioning of the HE sensor, relative permeability of the materials used, thickness of the moving part, etc. play a crucial role as far as the linearity of output and sensitivity are concerned. Sensor optimisation based on hard-ware implementation is time consuming, inefficient and less accurate. Hence, a finite element model of the sensor has been developed, and various studies have been conducted to optimise the parameters for best performance of the sensor. This also enables to achieve a linear output without using complex circuitry.

I. Introduction

Sensors find a large number of applications in contemporary automotive vehicles [1]. One such application is to monitor the amount of wear in an automotive brake shoe/pad unit [2], and provide an indication of the same to the vehicle operator. This will be very useful as it avoids the need of periodic manual inspection of the brake assembly, which is a very complex and time-consuming procedure, requiring expert manual intervention. Different techniques [3]-[11] are in vogue to sense the brake wear. Mechanical brake-lining-wear sensors [3], [4], which use a metal tab to generate a scraping sound once wear limit of a brake pad is reached, are being replaced by electronic wear sensors. Electronic wear sensors are developed using various principles. The variation in resistance/capacitance of a probe, which is embedded in the brake lining such that it wears out along with lining, was employed to indicate the wear condition in the schemes presented in [5], [6]. The need of brake pad replacement was detected in [7] by sensing the excessive travel of push-rod. Some of these techniques do not monitor brake wear continuously, while others require integration of a sensor at some of the jam-packed areas of the brake unit, which is not preferred.

Alternatively, an angle sensing principle can be used, especially for S-cam type air-brakes, to efficiently estimate the amount of brake wear. It involves the measurement of angular position of a cam-shaft, present in the brake assembly. The ends of this shaft are not easily accessible to install a sensor. Angle sensors [8], based on Magneto-Resistance (MR) or Hall Effect require a magnet to be placed at the center of the target's end, and hence cannot be employed for sensing the angle of the cam-shaft. Through-shaft angle sensing using an MR sensor and a gear unit has been presented in [9] and [10], but have short life-span due to wear associated with the gears. Also, it may have limited resolution, and requires complex circuitry to get a linear output. A scheme for continuous indication of cam-shaft position (and hence, brake wear) has been presented in [11]. It provides an adequate angular range and accuracy (of 1°). However, this scheme requires a magnetically coded circular disc and seven Hall sensors to resolve the angular position.

The basic idea of a simple, combined reluctance-Hall-Effect based angle sensor that can be used for through-shaft angle sensing has been reported [12]. It provides a linear output with-respect-to angle with good accuracy for a range of 220°. The output of the scheme is dependent upon parameters such as the position of the Hall Effect sensor in relation to other parts of the sensor unit, permeability of the materials employed in the reluctance part of the sensor, etc. In this paper, we perform an in-depth analysis (using finite element method) about the dependence of the output on these parameters, and thus optimizes the performance of the sensor. The details of the sensor unit and its characteristics, the procedure and the results obtained from the finite element analysis of the sensor are described in the following sections.

ISBN-10: 84-616-5438-2 | ISBN-13: 978-84-616-5438-3

II. Proposed Brake Wear Sensor Unit

A simplified diagram of a typical automotive brake assembly is shown in Figure 1. When the driver applies brake, the push-rod moves outward; rotating the Slack Adjuster (SA) and Cam-Shaft (CS). This rotates S-cam, which presses the brake-lining against the drum, causing the vehicle to stop. Brake-lining wears out with usage. As brake-lining wears, the SA automatically rotates by an angle θ with-respect-to CS, and retains that angle so that the driver need not press ahead the push-rod to a greater length (than in a normal case) while applying brake. Brake-wear can be monitored by measuring this angle, θ.

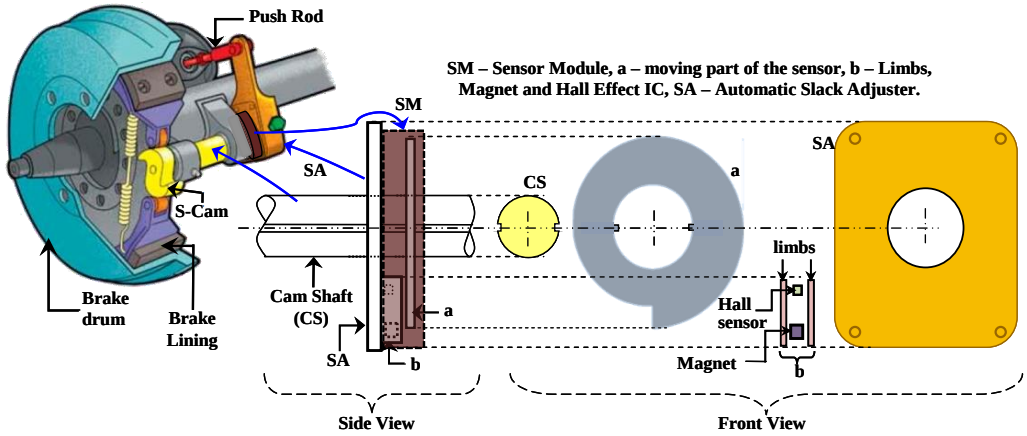

Figure 1. Schematic of a typical brake assembly is shown, with the proposed sensor module (SM) attached to it. Side and front views of SM is also shown. It consists of a rotating part 'a' and a fixed part 'b'. 'b', which is mounted on the slack adjuster, consists of two magnetic limbs, a NdFeB magnet and a Hall Sensor.

The angle θ is measured by the proposed sensor unit/module (SM) in the brake assembly, whose location is shown in Figure 1. It consists of two main parts 'a' and 'b'. As shown in Fig. 1, 'a' is a specially designed spiral shaped structure i. e., the Outer Radius (OD) of 'a' decreases with θ. It rotates along with CS. 'a' is fabricated from a Silicon steel sheet (0.3 mm thickness) by a standard wire-cutting process. The dimensions (inner diameter = 30 mm, minimum OD = 48 mm, maximum OD = 64 mm) of 'a' is selected to suit the size of a CS. Part 'b' is firmly fitted to the slack adjuster, SA. It has two parallel magnetic limbs that are separated by a small air-gap as shown in Figure 1 and also in the magnified view of the sensor in Figure 2. The dimensions of the limbs used were 30 mm × 10 mm × 3 mm. A rectangular shaped Neodymium magnet (with dimensions 10 mm × 10 mm × 2 mm) and a linear Hall Effect IC (SS49E from Honey Well Corp. [13]) are placed in the air-gap between the limbs as shown in Figure 2 (front view). 'a' rotates above 'b' with θ. Due to the spiral shape of 'a', portion of 'a' covering 'b' varies with θ. Thus, the magnetic field seen (and hence its output, v_H) by Hall sensor will change with θ.

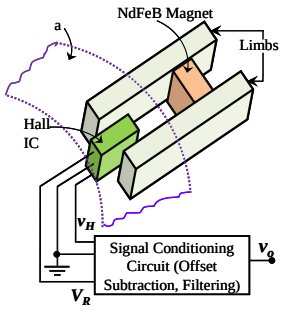

Figure 2. A 3-D view of the sensor unit.

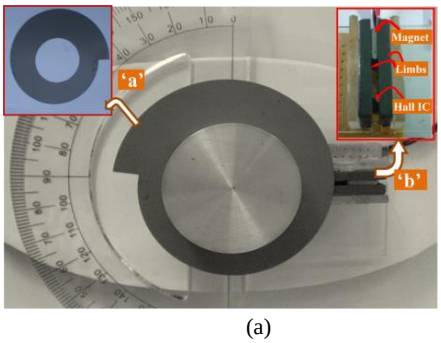

(a)

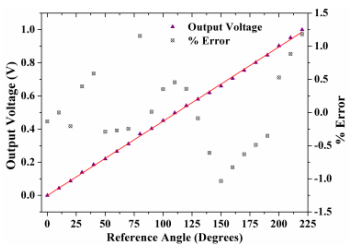

(b)

Figure 3. (a) Photograph of the prototype sensor unit built. Magnified view of the parts 'a' and 'b' are shown in inset. (b) Output voltage and Error characterisitics obtained from the sensor unit.

ISBN-10: 84-616-5438-2 | ISBN-13: 978-84-616-5438-3

A prototype of the sensor was developed. A photograph of the same is given in Figure 3 (a). Tests done on this unit showed that output v_H changes linearly with θ for a range of about 220°. This signal, v_H was given to a simple signal conditioning circuit, which subtracts the fixed bias voltage of the Hall sensor and filter out the high frequency disturbances present in v_H. Worst-case error observed in the resultant signal, v_o with-respect-to the sensing angle was less than 1.1 %. This is shown in the plot in Figure 3 (b).

A. Studies and Optimisation based on Finite Element Analysis (FEA) of the Sensor Model

A finite element model of the proposed sensor was developed to study and optimise its performance. The model was developed using COMSOL Multi-physics. A snap-shot of the model is shown in Figure 4. The directions of X, Y and Z axes are also shown in Figure 4. Limbs of part 'b' were realised using rectangular blocks having a μ_R (relative permittivity) of 50. Dimensions of limbs and the magnet used in FEA were chosen to match with the corresponding parts employed in the prototype sensor. Eight rectangular blocks (A_1–A_8) of width 1 mm was used to emulate the rotation of part 'a' above 'b' with θ. μ_R of individual blocks (A_1–A_8) were initially set to a higher value than that of part 'b' (μ_R = 500) to model θ = 0. A typical streamline plot of the magnetic flux density (say, B_{SEN}) seen by the Hall sensor for θ = 0° is also shown in Figure 4. Then, μ_R of A_1 is set to 1 to model an increase in θ. A further rotation of part 'a' is emulated by sequentially changing the permeability of these blocks (from A_2 to A_8) to 1. Hence, for θ = 360°, μ_R of all these blocks (A_1–A_8) will be set to 1. This basic model can be used to compute B_{SEN} for $\theta \in [0, 360°]$. Details of the FEA conducted using the above model, to analyse the effect of various parameters on the sensor output, is given below.

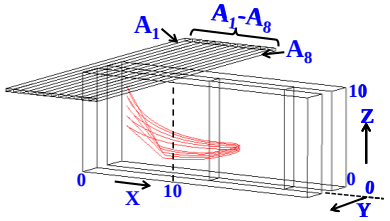

Figure 4. Comsol Model of the proposed sensor. Reference axes (X, Y and Z) are indicated, with the dimensions marked in mm. Rotation of part 'a' is emulated by varying the permeability of the blocks A_1-A_8. A typical streamline plot of B_{SEN} for θ = 0° is also shown.

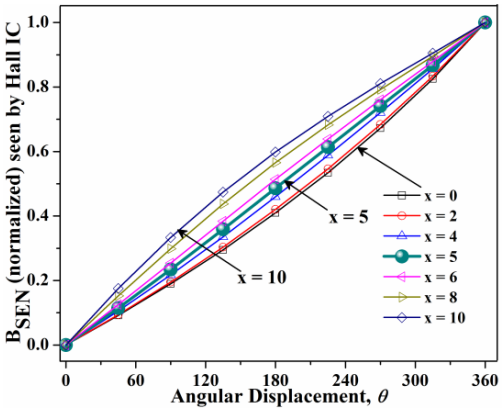

Figure 5. Family of magnetic flux density (B_{SEN}) vs angle θ characteristics obtained at z = 5 mm for x ϵ [0, 10 mm]. B_{SEN} has best linearity at x = 5mm.

(1) *Position P(x, y, z) of Hall Effect sensor*: As in Figure 2, the Hall sensor is located between the limbs, below the part 'a'. The linearity of the signals v_H and v_o, with respect to sensing angle θ, can change with the position of the Hall sensor. Hence, the best position (say, P_{BST}), at which best linearity is present, has to be determined for finalizing the Hall sensor position. To find P_{BST}, B_{SEN} was computed by the aforementioned procedure for $\theta \in$ (0-360°), at z = 5 mm, y = 0 mm for every x from 0 to 10 mm in steps of 0.2 mm, i. e., x ∈ (0, 10 mm). A family of B_{SEN} vs. θ curves obtained from this study is shown in Figure 5. Limited number of curves (better clarity) is shown in Figure 5. It can be seen from Figure 5 that B_{SEN} has best linearity when x = 5 mm.
Similar FEA was performed for positions P lying in the plane belonging to [x ∈ (0, 10 mm), y = 0, z ∈ (0, 10 mm)]. Worst-case Non-Linearity (WNL) of B_{SEN} vs. θ curve, for each P, has been calculated from FEA results, and is given in Figure 6(a). A 2-D projection of the Figure 6(a) is given in Figure 6(b) for better understanding. From Figure 6, we can generalize that the best linearity, in v_o, is observed near x = 5 mm, and lowest WNL is noted for z < 4 mm. Thus, for best performance, the Hall IC should be positioned at point P_{BST} (x→5 mm, y→0 mm, z ≤ 4 mm).

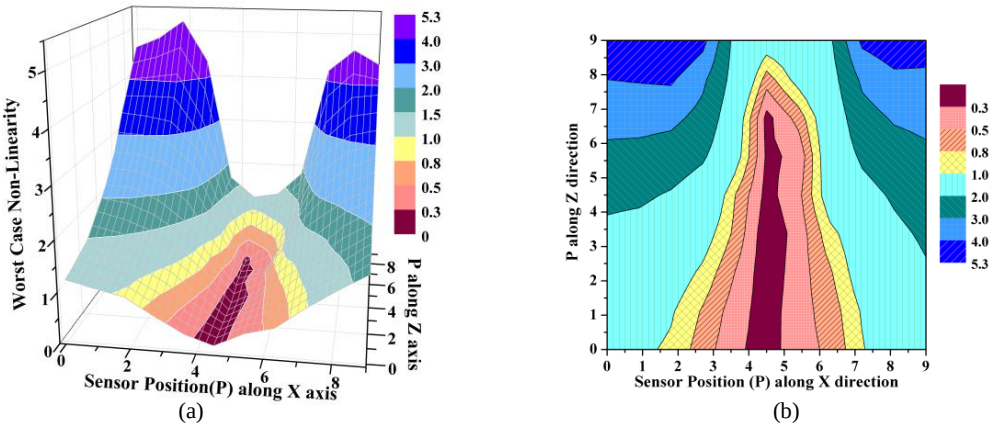

(a) (b)

Figure 6. (a) Variation of Worst-Case Non-linearity of the sensor output for different positions of Hall sensor. (b) A 2-D plot showing the projection of (a) on XZ plane. Position at which Hall IC has to be placed to get minimum non-linearity (over the required range) in v_o can be ascertained from these plots.

(2) *Thickness of 'a'*: The effect of thickness (t_A) of part 'a' on the non-linearity of v_o with-respect-to the sensing angle has been analysed for different sensor positions. First, B_{SEN} was computed by FEA for various t_A and for different positions P [$x \in (0, 10$ mm), $y = 0$, $z = 5$ mm]. Worst case Non-Linearity (WNL) was calculated for each case and given in Figure 7(a). It can be inferred from Figure 7(a) that, regardless of t_A, P_{BST} (best position) is near x = 5 mm. A similar FEA was conducted to compute WNL for different t_A and for sensor positions P [x = 3 mm, y = 0, $z \in (0, 10$ mm)]. The resulting plot of WNL with respect to t_A and z is given in Figure 7. From Figure 7, it can be seen that, for all $t_A \in [0.3$ mm, 0.9 mm], P_{BST} occurs for $z < 5$. Thus, from Figure 7 (a) and (b), we can infer that the point P_{BST} of best linearity is not much dependent on t_A. Shape of WNL curves, in Figure 7, does not alter much with t_A. Thus, for the sensor configuration analysed, the part 'a' can be fabricated from a material of thickness t_A, where $t_A \in [0.3$ mm, 0.9 mm]. The resultant change in non-linearity of B_{SEN} (or v_o) is very small.

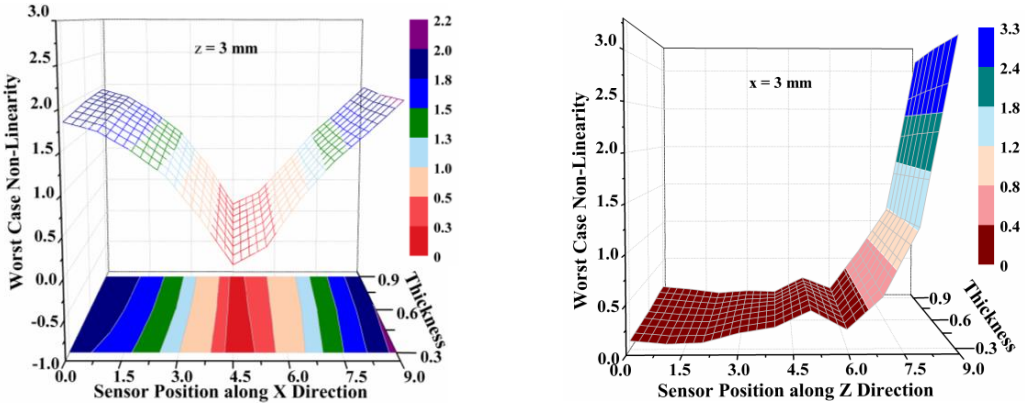

(a) (b)

Figure 7. (a) Plot of Worst-case Non-Linearity (WNL) for diferent thickness (t_A) of 'a' and different sensor positions P along X direction. (b) Variation of WNL w.r.t. t_A and P along Z direction.

(3) *Relative Permeability (μ_R) of 'a'*: The μ_R of the material, used to realise 'a' in the prototype shown in Figure 3 (a), was around 400. However, it varies with the material selected. An analysis has been carried out to ascertain the effect of different values of μ_R of 'a', where $\mu_R \in (40, 4000)$ on the non-linearity in output. The procedure is similar to that used in case (2). Figure 8(a) shows corresponding WNL pattern obtained for different values of μ_R and various sensor positions P [$x \in (0, 10$ mm), $y = 0$, $z = 5$ mm]. It can be seen from Figure 8 (a) that P_{BST} do not vary much with μ_R. The WNL plot obtained for different μ_R and different P along Z axis i.e. $P \in$ [x = 3 mm, y = 0, $z \in (0, 10$ mm)] is given in Figure 8 (b). From this plot, we can see that the region at which lowest WNL occurs is $z < 4$ mm. This is similar to the results obtained in (1) and (2). The effect of t_A and μ_R on WNL is similar as they play a similar role in determining the reluctance offered by part 'a'.

ISBN-10: 84-616-5438-2 | ISBN-13: 978-84-616-5438-3

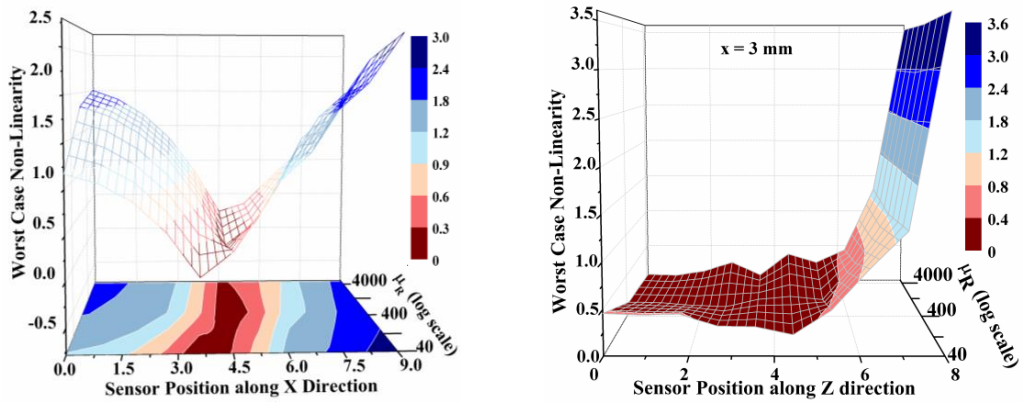

(a) (b)

Figure 8. (a) Plot of Worst-case Non-Linearity (WNL) for diferent permeability (μ_R) of 'a' and different sensor positions P along X direction. (b) Variation of WNL w.r.t. μ_R and P along Z direction.

III. Conclusions

A new sensor that measures angular position of a through shaft has been analysed. The proposed sensor can be used for brake-wear monitoring. The sensor analysed has a linear range of about 220°. The effect of position of Hall IC on linearity of the final output was studied using extensive finite element analysis, and the optimal region of placement of Hall IC for attaining best linearity was obtained. Similarly, the effect of variation in thickness and permeability of rotating part of the sensor unit was analysed. Based on these studies, the influence of these factors on the optimal position of Hall sensor and non-linearity in the output has been found. This information helps to substantially simplify the complexity of signal conditioning circuit employed, which is unavoidable otherwise, to obtain a linear output with respect to the sensing angle.

References

[1] W. J. Fleming, "Overview of automotive sensors," *IEEE Sensors J.*, vol. 1, no. 4, pp. 296-308, Dec 2001.
[2] Brake Pad Wear Sensors, Standard Motor Products Inc. [Online] Available: http://www.bwdbrand.com/upload/BWD/Documents/Library/BWDJTF_BRAKE-PAD-WEAR-SENSORS.PDF
[3] T. Maehara, "Audible Alarm Sounding Type Pad Clip Device for Disc Brake", *U. S. Patent* 4 124 105, 1978.
[4] D. F. Borkowski, "Lining Wear Sensor", *U. S. Patent* 4 250 978 1981.
[5] Gronowicz Jr., "Brake Pad Wear Sensor", *U. S. Patent* 6 302 241 2001.
[6] M. F. Passwater, "Brake Wear Sensor", *U. S. Patent* 2003/0006896 A1 2003.
[7] T. F. Runels, "Brake Actuator Service Limit Sensor", *U. S. Patent* 6 345 699 2002.
[8] C. P. O. Treutler, "Magnetic Sensors for Automotive Applications," *Sensors and Actuators A*, vol. 91, no. 1-2, pp. 2-6, Jun. 2001.
[9] Li Hao, Xu Yanliang, Zhang Yun, and Li Yuandong, "Development of Steering Wheel Angle Sensor Used for Torque Coordinating Control of In-wheel Motor Driven Electric Vehicle," in *Proc. IEEE ICEMS*, Beijing, China, Aug. 20–23, 2011, pp. 1-3.
[10] Schmitt et al., "Brake Lining Wear Sensor", *U. S. Patent* 7 808 374 2010.
[11] M. Ekeroth, "A brake lining wear indicating device", *European Patent* 0 830 521 B1 2001.
[12] C. S. Anoop, B. George, "A New Variable Reluctance-Hall Effect based Angle Sensor" in *Proc. IEEE ICST*, Kolkata, India, Dec.18-21, 2012, pp. 454-459.
[13] SS49E Series Linear Position Sensors, Honeywell Inc. [Online] Available: http://sccatalog.honeywell.com/imc/printfriendly.asp?FAM=solidstate&PN=SS49E